Joint Fixed Beamforming and Eigenmode Precoding for Super High Bit Rate Massive MIMO Systems Using Higher Frequency Bands

Tatsunori Obara†, Satoshi Suyama, Jiyun Shen, and Yukihiko Okumura

Research Laboratories, NTT DOCOMO, INC., 3-6 Hikari-no-oka, Yokosuka-shi, Kanagawa, 239-8536 Japan

E-mail: †tatsunori.obara.bh@nttdocomo.com

***Abstract*—In order to tackle rapidly increasing traffic, the 5th generation (5G) mobile communication system will introduce small cells using higher frequency bands with wider bandwidth to achieve super high bit rate transmission of several tens Gbps. Massive MIMO beamforming (BF) is one of promising technologies to compensate for larger path-loss in the higher frequency bands. Joint analog fixed BF and digital precoding has been proposed to reduce the cost of a Massive MIMO transceiver. However, the conventional scheme assumes the transmission of a few streams using well-known codebook-based precoding as the digital precoding, and both a selection method of the fixed BF weights and a digital precoder design, which are suitable for the super high bit rate transmission using multiple streams, have not been studied. This paper proposes a joint fixed BF and CSI-based precoding (called FBCP) scheme for the 5G Massive MIMO systems. FBCP first selects the analog fixed BF weights based on maximum total received power criterion, and then it calculates eigenmode (EM) precoding matrix exploiting CSI. This paper targets a 5G system achieving 20 Gbps in 20 GHz band as one example, and throughput performances of the proposed FBCP are evaluated by link level simulations and compared with those of the fixed BF and those of the EM precoding.**

Keywords—5G; higher frequency bands; Massive MIMO; analog fixed beamforming; eigenmode precoding.

I. INTRODUCTION

Against the rapid growing of mobile data traffic that the spread of smart phones and various mobile applications and services cause, higher-capacity transmission becomes urgent. 3GPP LTE Release 12 aiming at further improvement in frequency efficiency is being standardized [1], [2]. In order to prepare for the anticipated 1000-fold increase in the volume of data traffic in the next 10 years, dramatic performance enhancements in radio access technologies and networks are required for the 5th generation (5G) mobile communication networks beyond 2020 [3]. To realize the super high bit rate and large amount of capacity for the 5G, the Phantom Cell concept has been proposed [4], which is characterized by overlaying small cells using higher frequency bands onto a macro cell of an existing cellular system. The small cells provide the higher bit rate by the super wideband transmission using the higher frequency bands. For further increasing the bit rate in the small cells, enhanced MIMO technique is essential. In our previous work, the feasibility of 30 Gbps transmission was verified by computer simulations using 11 GHz band 24×24 MIMO channel data that are measured by outdoor experiments [5]. However, there is a problem that required total transmission power is over 30 dBm for applying the enhanced MIMO technique to the small cells using the higher frequency bands [6]. In order to overcome this problem, Massive MIMO that uses very large number of antennas [7], [8] is one of promising technologies for the super high bit rate 5G radio access [6].

Beamforming (BF) based on the Massive MIMO effectively compensates for the larger path-loss in the higher frequency bands. Eigenmode (EM) precoding using singular value decomposition (SVD) is one of well-known adaptive BF techniques, which requires channel state information (CSI) at the transmitter. However, the adaptive BF cannot be applied to reference signal (discovery signal [9]) transmission because CSI is not available at the transmitter. The transmission range of the reference signal is limited due to the large path-loss. Therefore, accurate CSI can be obtained only near a base station (BS) with the Massive MIMO. To overcome this problem, fixed BF, which uses the fixed BF weights selected from the BF weight candidates, can be introduced to the signal transmission. The digital fixed BF for digital baseband (BB) signals requires the same number of BB chains as the number of transmitter antennas, which significantly increases the cost of the Massive MIMO transceiver. On the other hand, in the analog fixed BF for the analog radio frequency (RF) signals, the number of the BB chains can be limited to the number of digital precoder outputs, which results in the cost reduction. In [10]-[12], joint processing of the analog fixed BF and the digital precoding, which is referred as to hybrid BF, has been proposed to reduce the cost of the Massive MIMO transceiver. The hybrid BF technique in [12] employs the analog fixed BF and codebook-based precoding, and the analog BF weights and the precoding matrix are jointly optimized by exhaustive search based on the maximum channel capacity criterion. However, it assumes the hybrid BF for the transmission of one or two streams, and thus joint processing (hybrid BF) suitable for the super high bit rate transmission using multiple streams has not been studied sufficiently.

This paper proposes joint processing of the analog fixed BF and CSI-based precoding (called FBCP) for the 5G super high bit rate Massive MIMO systems using the higher frequency bands. The proposed FBCP first selects the analog fixed BF weights whose number is larger than the number of the streams and much less than the number of transmitter antennas based on maximum total received power criterion. Next, it calculates the EM precoding matrix based on SVD of an equivalent channel matrix (CSI) that is multiplied the channel matrix by the selected analog fixed BF weights. Throughput performances of the FBCP are evaluated by link level simulations that target 20 Gbps transmission in 20 GHz band as one example, and it is shown that the proposed FBCP with 256 transmitter antennas and 28 BB chains can achieve almost the same throughput as the fully digital Massive MIMO which employs the EM precoding with 256 transmitter antennas.

II. MASSIVE MIMO USING PROPOSED FBCP

A. Transmitter and Receiver Structure

Fig. 1(a) shows the Massive MIMO transmitter structure employing the joint analog BF and the digital precoding. This paper considers a downlink MIMO-OFDM system that employs the conventional MIMO receiver as shown in Fig. 1(b) due to the size of user equipment. The numbers of transmitter antennas, receiver antennas, spatially multiplexed data streams, and BB chains are denoted as N_T, N_R, M, and L ($\geq M$), respectively. In the case of $L = N_T$, the structure excluding the analog BF in Fig. 1(a) is equivalent to a fully digital Massive MIMO transmitter. To reduce the cost of the Massive MIMO transmitter, L is assumed to be much smaller than N_T. As the transmitter and receiver antenna configuration, this paper employs uniform planar array shown in Fig. 2. Let Δx and Δz denote transmitter or receiver antenna spacing in horizontal and vertical axes, respectively, and ϕ and θ are azimuth and zenith angles of departure or arrival. At the transmitter, M data streams at each subcarrier are precoded and converted into L precoded signals. After inverse fast Fourier transform (IFFT) and digital-to-analog conversion (DAC), the analog BF is applied to L analog precoded signals. The analog BF consists of LN_T variable phase shifters, power amplifiers, and N_T adders. At the receiver, the received signal is sampled by analog-to-digital converter (ADC), and after FFT, the postcoding is applied to the received signal at each subcarrier to separate the M data streams.

Now, let $\mathbf{H}(n)$, $\mathbf{P}(n)$, and $\mathbf{B}(n)$ denote an $N_R \times N_T$ MIMO channel matrix, an $L \times L$ precoding matrix, and an $N_R \times N_R$ postcoding matrix, respectively. An $N_R \times 1$ postcoded received signal vector at the nth subcarrier can be expressed as

$$\mathbf{y}(n) = \mathbf{B}(n)\mathbf{H}(n)\mathbf{W}\mathbf{P}(n)\mathbf{s}(n) + \mathbf{B}(n)\mathbf{z}(n), \qquad (1)$$

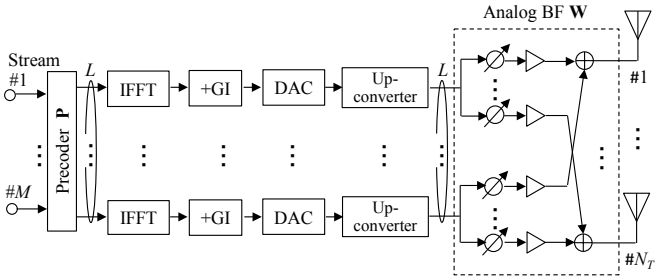

(a) Transmitter

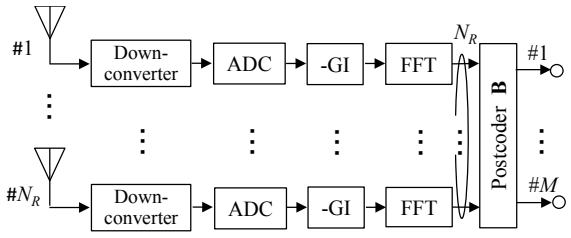

(b) Receiver

Fig. 1. System model of Massive MIMO using FBCP.

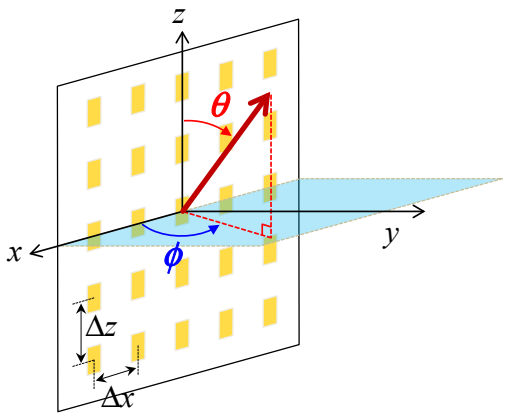

Fig. 2. Uniform planar array.

where $\mathbf{s}(n)$ is an $L \times 1$ transmitted signal vector given by

$$\mathbf{s}(n) = [\mathbf{d}^{\mathrm{T}}(n) \quad \mathbf{0}^{\mathrm{T}}]^{\mathrm{T}}. \qquad (2)$$

$\mathbf{d}(n)$ and $\mathbf{0}$ are an $M \times 1$ transmitted signal vector and an $(L-M) \times 1$ zero vector, respectively. $(.)^{\mathrm{T}}$ denotes the transposition. $\mathbf{z}(n)$ is an $N_R \times 1$ noise vector. $\mathbf{W}$ is an $N_T \times L$ analog BF weight matrix given by

$$\mathbf{W} = [\mathbf{w}_1 \ \ \mathbf{w}_2 \ \ \ldots \ \ \mathbf{w}_L], \qquad (3)$$

where $\mathbf{w}_l$ ($l = 1 \sim L$) is an $N_T \times 1$ analog BF weight vector (analog BF weights) for the lth precoded OFDM signal. Note that multiplying the precoded signal $\mathbf{P}(n)\mathbf{s}(n)$ by the BF weight matrix $\mathbf{W}$ is realized by the phase shifters and the power amplifiers, and that the same analog BF weight matrix $\mathbf{W}$ is used for all the subcarriers.

B. Analog fixed BF weights and precoding matrix for FBCP

As the analog BF weight vector, the proposed FBCP employs an $N_T \times 1$ steering vector at the transmitter antenna array. Let N_{Tx} and N_{Tz} denote the numbers of antennas in the horizontal and vertical axes of Fig. 2, respectively, and the steering vector is given by

$$\mathbf{w}^{\mathrm{T}}(\phi,\theta) = \frac{1}{\sqrt{N_T}}\Big[\exp\{-jW_{0,0}(\phi,\theta)\} \ldots \exp\{-jW_{N_{Tx}-1,0}(\phi,\theta)\} \ldots \exp\{-jW_{0,N_{Tz}-1}(\phi,\theta)\} \ldots \exp\{-jW_{N_{Tx}-1,N_{Tz}-1}(\phi,\theta)\}\Big], \qquad (4)$$

where $W_{n_x,n_z}(\phi,\theta)$ is the phase rotation at the (n_x, n_z)-th element of the transmitter antenna array and $n_x = 0 \sim N_{Tx}-1$, $n_z = 0 \sim N_{Tz}-1$. In addition, $W_{n_x,n_z}(\phi,\theta)$ is expressed as

$$W_{n_x,n_z}(\phi,\theta) = \frac{2\pi}{\lambda}(n_x \Delta x \cos\phi \sin\theta + n_z \Delta z \cos\theta), \qquad (5)$$

where λ is the wavelength of the carrier frequency.

The proposed FBCP employs a successive two-stage algorithm. Firstly, L optimum analog fixed BF weights are selected from some analog fixed BF weight candidates. Then, the EM precoding and postcoding matrices are calculated by SVD using the channel matrix and the L selected analog fixed BF weights.

In the first stage, L optimum analog fixed BF weights are selected based on maximum total received power criterion. Since the square-root of sum of eigenvalues in the channel correlation matrix, which is generated from the equivalent channel matrix $\mathbf{H}(n)\mathbf{W}$, is equivalent to Frobenius norm of $\mathbf{H}(n)\mathbf{W}$ (i.e., the total received power), the FBCP employs the maximum total received power criterion as simple solution in the first stage. As the analog fixed BF weight candidates for each BB chain, $\mathbf{w}(n_\phi\Delta\phi, n_\theta\Delta\theta)$ in (4) in the discrete azimuth and zenith angles of $n_\phi\,\Delta\phi$ and $n_\theta\,\Delta\theta$ is used, and $n_\phi = 0\sim N_\phi-1$ and $n_\theta = 0\sim N_\theta-1$, where $\Delta\phi$ and $\Delta\theta$ are search angular intervals in the azimuth and zenith angles, $N_\phi = 180/\Delta\phi$ and $N_\theta = 180/\Delta\theta$. The FBCP selects the optimum analog fixed BF weight from the $N_\phi N_\theta$ candidates for the lth BB chain, and the selected analog fixed BF weight for each BB chain should be different each other. Hence, the optimum analog fixed BF weight for the lth BB chain is given by

$$\mathbf{w}_l = \mathbf{w}(n_\phi^{opt}\Delta\phi, n_\theta^{opt}\Delta\theta) \ , \tag{6}$$

$$(n_\phi^{opt}, n_\theta^{opt}) = \arg\max_{n_\phi, n_\theta} \left\| \mathbf{H}(n)\mathbf{w}(n_\phi\Delta\phi, n_\theta\Delta\theta) \right\|^2 \ , \tag{7}$$

$$\mathbf{w}_l \neq \mathbf{w}_{l-1} \neq \ldots \neq \mathbf{w}_1 \ , \tag{8}$$

where $\|.\|$ denotes the norm of vector. The discovery signal is transmitted with the analog fixed BF using $\mathbf{w}(n_\phi\Delta\phi, n_\theta\Delta\theta)$ and without the CSI-based precoding, i.e. $\mathbf{P}(n) = \mathbf{I}$ where $\mathbf{I}$ is the identity matrix of size L. At the receiver, the norm of $\mathbf{H}(n)\mathbf{w}(n_\phi\Delta\phi, n_\theta\Delta\theta)$ is calculated from the received power of the discovery signal, and then, the optimum analog fixed BF weight $\mathbf{w}_l$ is selected by (6) and (7). The information on the selected BF weight, n_ϕ^{opt} and n_θ^{opt}, for the L BB chains are fed back to the transmitter. Note that the optimum BF weight is selected from the $N_\phi N_\theta$ candidates, and hence the BF weight selection should be performed at a few subcarriers. In this paper, only one subcarrier is used for the BF weight selection.

Moreover, the equivalent channel matrix $\mathbf{H}(n)\mathbf{W}$ is estimated by exploiting the reference signal with the selected analog fixed BF.

In the second stage, the precoding matrix $\mathbf{P}(n)$ and the postcoding matrix $\mathbf{B}(n)$ are generated by exploiting the estimated $\mathbf{H}(n)\mathbf{W}$ at each subcarrier. The SVD of $\mathbf{H}(n)\mathbf{W}$ can be written as

$$\mathbf{H}(n)\mathbf{W} = \mathbf{U}(n)\mathbf{D}(n)\mathbf{V}^{\mathrm{H}}(n) \ , \tag{9}$$

where $(.)^{\mathrm{H}}$ denotes the Hermitian transposition and $\mathbf{U}(n)$ and $\mathbf{V}(n)$ are the $N_R\times N_R$ and $L\times L$ unitary matrices, respectively. $\mathbf{D}(n)$ is the $N_R\times L$ diagonal matrix whose diagonal elements consist of singular values of $\mathbf{H}(n)\mathbf{W}$. Thus, $\mathbf{P}(n)$ and $\mathbf{B}(n)$ are respectively chosen as

$$\begin{cases} \mathbf{P}(n) = \mathbf{V}(n) \\ \mathbf{B}(n) = \mathbf{U}^{\mathrm{H}}(n) \end{cases} . \tag{10}$$

Then, (1) can be rewritten as

$$\begin{aligned} \mathbf{y}(n) &= \mathbf{U}^{\mathrm{H}}(n)\mathbf{H}(n)\mathbf{W}\mathbf{V}(n)\mathbf{s}(n) + \mathbf{U}^{\mathrm{H}}(n)\mathbf{z}(n) \\ &= \mathbf{D}(n)\mathbf{s}(n) + \mathbf{U}^{\mathrm{H}}(n)\mathbf{z}(n) \end{aligned} \ , \tag{11}$$

and the M streams can be easily detected.

III. Computer Simulations

A. Simulation Conditions

Link level simulations are performed to evaluate the performances of the 20 Gbps Massive MIMO employing the proposed FBCP. The simulation conditions are given in Table I. The carrier frequency and the bandwidth are set to 20 GHz and 400 MHz, respectively. N_T is set to 16, 64, and 256, and N_R is fixed to 16. Transmission power per stream and total transmission power are constant regardless of N_T. The number of the streams, M, is fixed to 16 to achieve 20 Gbps. Hence, rank adaptation is not applied. The turbo code with coding rate R is used as channel coding, and adaptive modulation and coding (AMC) is also employed. The maximum bit rate reaches 23.5 Gbps when the modulation and coding scheme is 64QAM and R = 3/4. In order to keep the entire antenna size of the uniform planar array, the transmitter antenna spacing Δx (= Δz) is set to 2λ, 1λ, and 0.5λ for N_T = 16, 64, and 256, respectively. Spatially correlated MIMO channel is based on Kronecker model, where transmitter and receiver spatial correlation matrices are generated by the power angular spectrum with Laplacian distribution [13], [14]. We assume the 16-path Nakagami-Rice fading channel with Rician factor, K, = 10 dB. Ideal estimation for CSI is also assumed.

TABLE I
Simulation Conditions

Transmission scheme	MIMO-OFDM
Carrier frequency	20 GHz
Bandwidth	400 MHz
No. of active subcarriers	Pilot: 32, data: 2000
No. of antennas	Transmitter: N_T = 16, 64, 256 Receiver: N_R = 16
No. of streams, M	16
Data modulation	QPSK, 16QAM, 64QAM (w/ AMC)
Channel coding	Turbo coding with coding rate R = 1/2, 2/3, 3/4 (w/ AMC)
Antenna array structure	Uniform planar array
Antenna spacing	Transmitter: 2λ, 1λ, 0.5λ Receiver: 0.5λ
MIMO channel	Kronecker model
Power angular spectrum	Laplacian distribution
Average angle (azimuth, zenith)	Departure: (90 deg., 90 deg.) Arrival: (90 deg., 90 deg.)
Angular spread (azimuth, zenith)	Departure: (5 deg., 5 deg.) Arrival: (20 deg., 20 deg.)
Fading channel	16-path Nakagami-Rice fading with K = 10 dB
CSI estimation	Ideal

B. Optimization of Number of BB Chains, L

The number of the BB chains, L, and the search angular intervals, $\Delta\phi$ and $\Delta\theta$, should be jointly optimized by the simulations. For simplicity, the optimization of L is firstly carried out for the given $\Delta\phi$ and $\Delta\theta$ in this section, and then the optimum $\Delta\phi$ and $\Delta\theta$ are evaluated for the given L in Sect. III-C. Fig. 3 shows throughput performances of the FBCP with L. The average signal-to-noise power ratio (SNR) is fixed to 35 dB, and $\Delta\phi$ and $\Delta\theta$ are assumed to be 5 degrees. For

comparison, throughput performances of the EM precoding (called EM), which employs the fully digital Massive MIMO of $N_T = L$, are also plotted in Fig. 3. It is shown that as L increases, the throughput of the FBCP increases and approaches to that of EM by improvement of the BF gain. The minimum values of L for $N_T = 64$ and 256 to obtain the maximum throughput are 34 and 28, respectively. That is to say, L can be reduced as N_T increases. On the other hand, EM requires the same number of the BB chains as N_T, and thus FBCP is the much cost-effective scheme in comparison with EM.

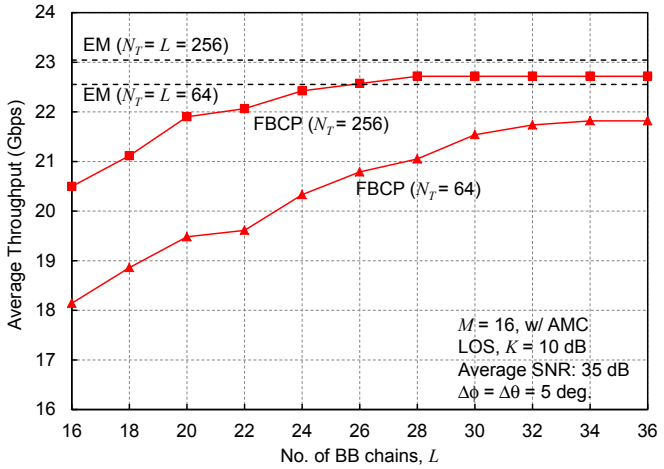

Fig. 3. Optimization of L.

C. Optimization of Search Angular Intervals, $\Delta\phi$ and $\Delta\theta$

Fig. 4 shows throughput performances of the FBCP with the BF weight search angular intervals, $\Delta\phi$ and $\Delta\theta$, when the average SNR is 35 dB. We assume $\Delta\phi = \Delta\theta$ for simplicity. L for $N_T = 64$ and 256 are set to 34 and 28, respectively. It can be seen from Fig. 4 that the optimum search interval, $\Delta\phi$ ($\Delta\theta$), to maximize the throughput for $N_T = 64$ and 256 are 11 degrees and 5 degrees, respectively. Note that the optimum $\Delta\phi$ and $\Delta\theta$ depend on the parameters of the channel model such as angular spread.

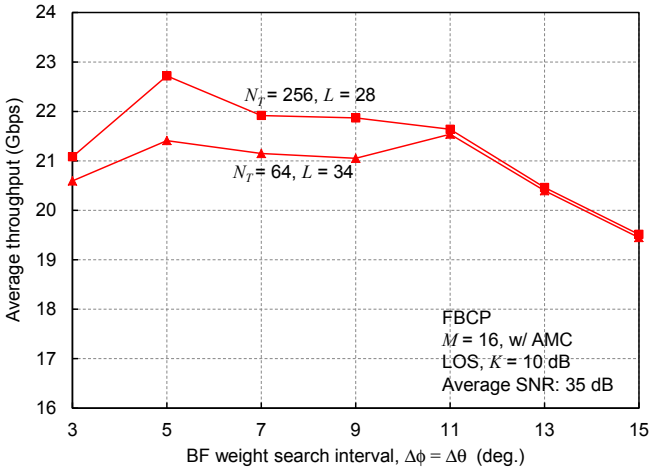

Fig. 4. Optimization of $\Delta\phi$ and $\Delta\theta$.

D. Throughput Performances of Massive MIMO Using FBCP

Fig. 5 shows throughput performances of the Massive MIMO using the FBCP. Also, throughput performances of EM and those of the analog fixed BF with the MMSE detection are plotted in Fig. 5 for comparison. From Figs. 3 and 4, the FBCP employs the optimized parameter set of L = 34, $\Delta\phi = \Delta\theta = 11$ degrees and L = 28, $\Delta\phi = \Delta\theta = 5$ degrees for $N_T = 64$ and 256, respectively. Fig. 5 shows that EM with $N_T = 64$ and 256 achieves the higher throughput than $N_T = 16$ by exploiting the higher BF and diversity gains. On the other hand, the proposed FBCP with $N_T = 64$ and 256 achieves the 20 Gbps throughput at average SNR of 30 dB and 24 dB, respectively, and the throughput performance of the FBCP is almost the same as that of EM in the average SNR region of more than 30 dB. It is also shown that the FBCP with $N_T = 256$ (64) can limit the SNR degradation from EM to achieve the 20 Gbps throughput to 4 dB (3 dB) in spite of the significantly low complexity. In the analog fixed BF with the MMSE detection, the throughput performance drastically degrades compared to the FBCP and EM, because the analog fixed BF generates the correlated channel with the BF gain and the MMSE detection cannot completely extract the M streams from the channel. This result indicates that the combination of the analog fixed BF and the digital precoding with L ($\geq M$) is essential for achieving the super high bit rate in the Massive MIMO. Note that in comparison with the conventional MIMO using the EM with $N_T = 16$, the FBCP with $N_T = 64$ and 256 can reduce the required SNR at the 20 Gbps throughput by 7 dB and 13 dB, respectively.

In addition, Fig. 5 shows that the FBCP achieves the slightly higher throughput than EM in the low SNR region. To clarify this reason, cumulative distribution function (CDF) of the eigenvalue in each EM channel is shown in Fig. 6. From Fig. 6, upper eigenvalues of the FBCP are larger than those of EM while lower eigenvalues are smaller than those of EM. In the low SNR region, the throughput performance mainly depends on the upper eigenvalues, and thus, the FBCP achieves the higher throughput than EM. In the high SNR region, the lower eigenvalues also make an influence on the throughput. However, the performance degradation of the FBCP can be reduced by increasing L as shown in Fig. 3.

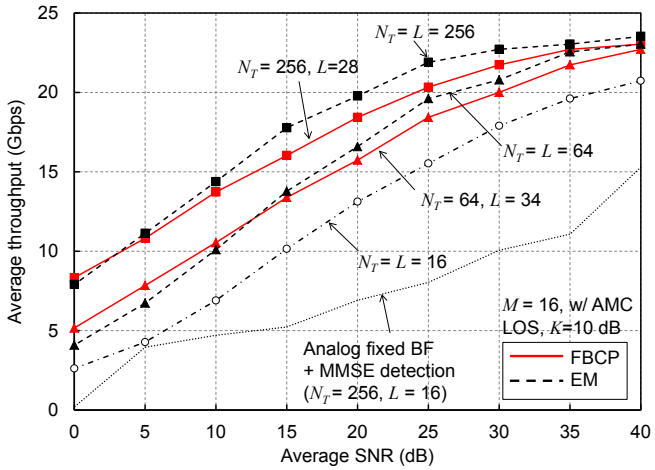

Fig. 5. Throughput performances of Massive MIMO using FBCP.

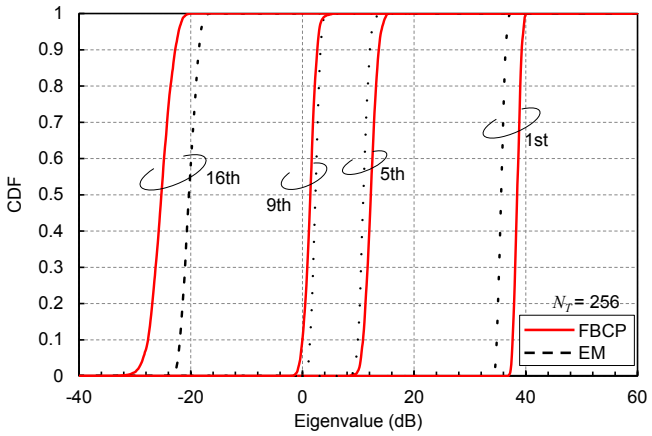

Fig. 6. CDF of eigenvalues.

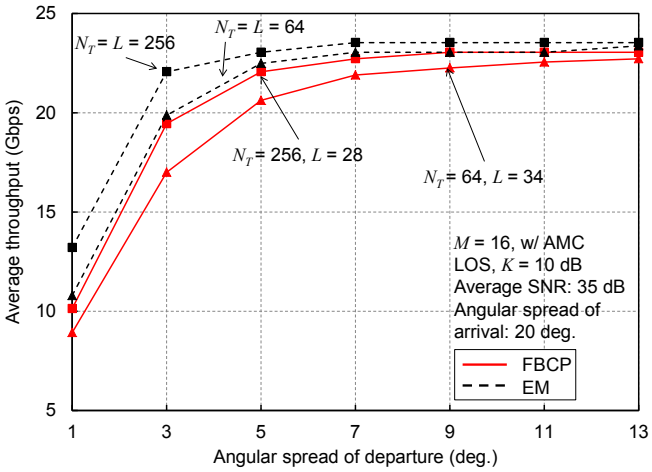

Fig. 7 Impact of ASoD.

Throughput performances of the FBCP and the EM are depicted in Fig. 7 as a function of the angular spread of departure (ASoD), when the average SNR is 35 dB and the angular spread of arrival is fixed to 20 degrees. It can be seen from Fig. 7 that the throughput performance improves as the ASoD becomes larger. In the case of the EM, the throughput performance approaches to the maximum value when the ASoD is equal to or larger than 7 degrees. On the other hand, when the ASoD is equal to or larger than 11 degrees and 9 degrees, the FBCP schemes with N_T = 64 and 256 achieve almost the maximum throughput, respectively, and the throughput of the FBCP is almost the same as that of the EM.

IV. Conclusion

This paper proposed joint processing of analog fixed BF and CSI-based precoding (called FBCP) suitable for the super high bit rate Massive MIMO transmission using multiple streams in higher frequency bands. The proposed FBCP first selects the analog fixed BF weights whose number is larger than the number of the streams based on maximum total received power criterion, and then it calculates the EM precoding matrix based on SVD of an equivalent channel matrix that is multiplied the channel matrix by the selected analog fixed BF weights. Throughput performances of the proposed FBCP were evaluated by link level simulations of 20 GHz band 20 Gbps transmission. The simulation results showed that the FBCP with 256 transmitter antennas and 28 BB chains can limit the SNR degradation from the fully digital Massive MIMO with the EM precoding to 4 dB at the 20 Gbps throughput in spite of the significantly low complexity. We showed that the FBCP with 256 transmitter antennas can achieve the higher throughput than the conventional MIMO with 16 transmitter antennas, and that the required SNR to achieve the throughput of 20 Gbps can be reduced by 13 dB.

Acknowledgment

Part of this work has been performed in the framework of the FP7 project ICT-317669 METIS, which is partly funded by the European Union. The authors would like to acknowledge the contributions of their colleagues in METIS, although the views expressed are those of the authors and do not necessarily represent the project.

References

[1] 3GPP, TR 36.932 (V12.1.0), "Scenarios and requirements for small cell enhancements for E-UTRA and E-UTRAN," March 2013.

[2] 3GPP, TR 36.872 (V0.3.0), "Small cell enhancements for E-UTRA and E-UTRAN - physical aspects," May 2013.

[3] 3GPP, RWS-120010, NTT DOCOMO, "Requirements, candidate solutions & technology roadmap for LTE Rel-12 Onward," June 2012.

[4] H. Ishii, Y. Kishiyama, and H. Takahashi, "A novel architecture for LTE-B, C-plane/U-plane split and phantom cell concept," IEEE GLOBECOM2012 Workshop, Dec. 2012.

[5] S. Suyama, J. Shen, H. Suzuki, K. Fukawa, and Y. Okumura, "Evaluation of 30 Gbps super high bit rate mobile communications using channel data in 11 GHz band 24x24 MIMO experiment," IEEE ICC2014, June 2014.

[6] S. Suyama, J. Shen, A. Benjebbour, Y. Kishiyama, and Y. Okumura, "Super high bit rate radio access technology for small cells using higher frequency bands," IEEE IMS2014, June 2014.

[7] T. L. Marzetta, "Non-cooperative cellular wireless with unlimited numbers of base station antennas," IEEE Trans. Wireless Commun., vol. 9, no. 11, Nov. 2010.

[8] F. Rusek, D.Persson, L. K. Buon, E. G. Larsson, T. L. Marzetta, O. Edfors, and F. Tufvesson, "Scaling up MIMO: opportunities and challenges with very large arrays," IEEE Signal Processing Magazine., vol. 30, no. 1, pp. 40-60, January 2013.

[9] 3GPP, R1-140622, NTT DOCOMO, "Views on discovery signal design for Rel-12 small cell enhancements," Feb. 2014.

[10] O. E. Ayach, R. W. Heath, S. Abu-Surra, S. Rajagopal, Z. Pi, "Low complexity precoding for large millimeter wave MIMO system," IEEE ICC2012, June, 2012.

[11] J. Brady, N. Behdad, and A. Sayeed, "Beamspace MIMO for millimeter-wave communications: system architecture, modeling, analysis, and measurements," IEEE Trans. Antennas Propag., vol. 61, no. 7, pp. 3814-3827, July, 2013.

[12] T. Kim, J. Park, J. Seol, S. Jeong, J. Cho, and W. Roh, "Tens of Gbps support with mmWave beamforming systems for next generation communications," IEEE GLOBECOM2013, Dec. 2013.

[13] IEEE 802.11-03/940r4, "TGn channel models," May 2004.

[14] 3GPP, TR 36.873 (V1.0.0), "3D channel model for LTE (release 12)," Sept. 2013.